

2016 MARS INSIGHT MISSION DESIGN AND NAVIGATION

**Fernando Abilleira[†], Ray Frauenholz^ψ, Ken Fujii*,
Mark Wallace[§], Tung-Han You[^]**

Scheduled for a launch in the 2016 Earth to Mars opportunity, the Interior Exploration using Seismic Investigations, Geodesy, and Heat Transport (InSight) Mission will arrive to Mars in late September 2016 with the primary objective of placing a science lander on the surface of the Red Planet followed by the deployment of two science instruments to investigate the fundamental processes of terrestrial planet formation and evolution. In order to achieve a successful landing, the InSight Project has selected a launch/arrival strategy that satisfies the following key and driving requirements: (1) Deliver a total launch mass of 727 kg, (2) target a nominal landing site with a cumulative ΔV_{99} less than 30 m/s, and (3) approach EDL with a V-infinity upper limit of 3.941 km/s and (4) an entry flight-path angle (EFPA) of -12.5 ± 0.26 deg, 3-sigma; the InSight trajectories have been designed such that they (5) provide UHF-band communications via Direct-To-Earth and MRO from Entry through landing plus 60 s, (6) with injection aimpoints biased away from Mars such that the probability of the launch vehicle upper stage impacting Mars is less than 1.0×10^{-4} for fifty years after launch, and (7) non-nominal impact probabilities due to failure during the Cruise phase less than 1.0×10^{-2} .

INTRODUCTION

The Interior Exploration using Seismic Investigations, Geodesy, and Heat Transport (InSight) mission will deliver a lander to the surface of Mars during the 2016 Earth to Mars opportunity. The overall scientific goal of the mission is to address one of the most fundamental issues of planetary and solar system science, understanding the processes that shaped the rocky planets of the inner solar system, including Earth, more than four billions years ago. The InSight spacecraft will be launched in March 2016 from the Western Test Range (WTR) at Vandenberg Air Force Base (VAFB) on an Atlas V 401 launch vehicle and will arrive to Mars in September 28, 2016. The primary systems of the InSight Project consist of a flight system, a launch vehicle, and the terrestrial ground system to conduct mission operations, including the collection and processing of data. The flight system consists of an Earth-Mars stage, and Entry, Descent, and Landing (EDL) package, and a science lander carrying two science instrument packages and an instrument deployment system¹.

MISSION

Launch

InSight will be launched into a ballistic, Type 1 trajectory during a 23-day launch period extending from March 4 through March 26, 2016. The launch window on any given day during the launch period will have a duration of up to 120 min. The launch vehicle injection targets are specified as the hyperbolic injection energy per unit mass (C3), Declination of the Launch Asymptote (DLA), and Right ascension of the

[†] InSight Mission Design and Navigation Manager, Fernando.Abilleira@jpl.nasa.gov.

^ψ InSight Maneuver Analyst, Raymond.B.Frauenholz@jpl.nasa.gov.

* InSight Mission Planner, Kenneth.K.Fujii@jpl.nasa.gov.

[§] InSight Trajectory Lead, Mark.S.Wallace@jpl.nasa.gov.

[^] InSight Navigation Lead, Tung-Han.You@jpl.nasa.gov.

Jet Propulsion Laboratory, California Institute of Technology, 4800 Oak Grove Drive, Pasadena, CA 91109.

Launch Asymptote (RLA) at the Targeting Interface Point (TIP). The Maximum Possible Value (MPV) of the spacecraft mass is 727 kg which corresponds to a maximum C3 of $47.1 \text{ km}^2/\text{s}^2$ for a launch on an Atlas V 401 for DLAs between $+28.5 \text{ deg}$ and -28.5 deg . Note that launch vehicle performance degradation due to the high launch DLAs is expected. InSight has a constant arrival day of September 28th, 2016 which greatly simplifies mission operations planning².

Interplanetary Cruise

During the 6.5-month interplanetary flight, up to six Trajectory Correction Maneuvers (TCMs) will be executed to remove launch vehicle dispersions, planetary biasing, and deliver the spacecraft to the optimal entry aimpoint which is defined to be at a Mars radius of 3522.2 km. Figure 1 illustrates the interplanetary trajectory in heliocentric form. During the interplanetary cruise both engineering and instrument checkouts will take place to ensure the system performs as expected during cruise, EDL, and surface operations.

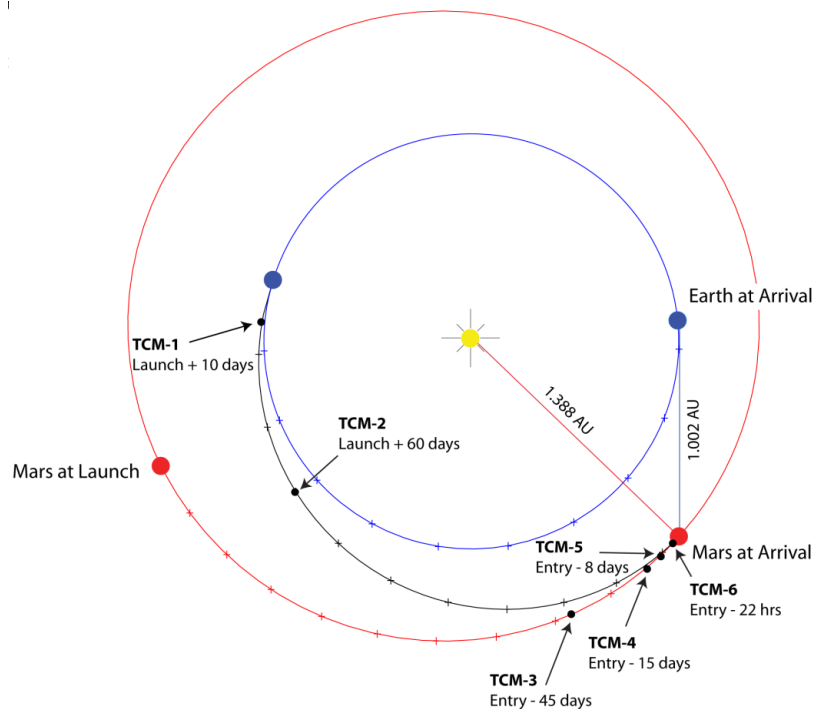


Figure 1. Interplanetary Trajectory for Launch Period Open (03/04/2016)

The approach subphase includes the acquisition and processing of navigation data needed to support the development of the final four TCMs, the spacecraft activities leading up to a separation of the entry vehicle from the cruise stage, and the final turn to entry attitude. The last four TCMs are used to perform final adjustments to the incoming trajectory at Mars to ensure that the desired entry conditions are achieved. All other spacecraft activities, particularly those that could influence the spacecraft's trajectory such as spacecraft attitude turns, are minimized. During this subphase, the amount of requested DSN tracking is substantially increased to allow more accurate trajectory solutions to be determined in the final weeks before Mars arrival. In addition to increased Doppler and ranging data, additional Delta Differential One-Way Ranging (Δ DOR) measurements are also taken during this period to ensure an accurate delivery at Mars¹.

Several days prior to Entry, the EDL sequence is loaded on-board the spacecraft and begins executing. This sets a clock running which will bring about the sequence of activities that enable the EDL phase. A final TCM opportunity, along with a contingency TCM during the last 24 hours, may be used to make the final corrections to target the Mars atmospheric Entry Interface Point (EIP). At approximately seven minutes prior to encountering the Martian atmosphere, the Cruise stage is jettisoned from the entry vehicle, and communication via UHF to Earth via the Mars Reconnaissance Orbiter (MRO) will begin.

Entry, Descent, and Landing

Six and a half minutes before entering into the Martian atmosphere, the entry vehicle begins its turn to entry attitude. Following atmospheric entry, the vehicle rapidly decelerates due to drag from its hypersonic entry velocities to supersonic parachute deployment velocities as it passes through the increasingly dense atmosphere. The Guidance, Navigation, and Control (GNC) flight software controls the vehicle during this time and provides a trigger to deploy the parachute at a targeted velocity of Mach 1.56. The heatshield is jettisoned after the parachute has opened, followed later by the power up of the landing radar and the deployment of the landing legs. The radar will be used during the terminal descent phase to provide input to the descent engines that are then fired in a sequence that allows the spacecraft to slow down and land gently on the Martian surface. Figure 2 shows the location of Elysium Planitia where all four current candidate landing sites reside, along with the landing sites for Viking, Mars Pathfinder, Spirit, Opportunity, Phoenix, and Curiosity. The final four ellipses are illustrated in Figure 3. Note that all the InSight candidate landing sites are located within a latitude range between 5°N to 3°N³.

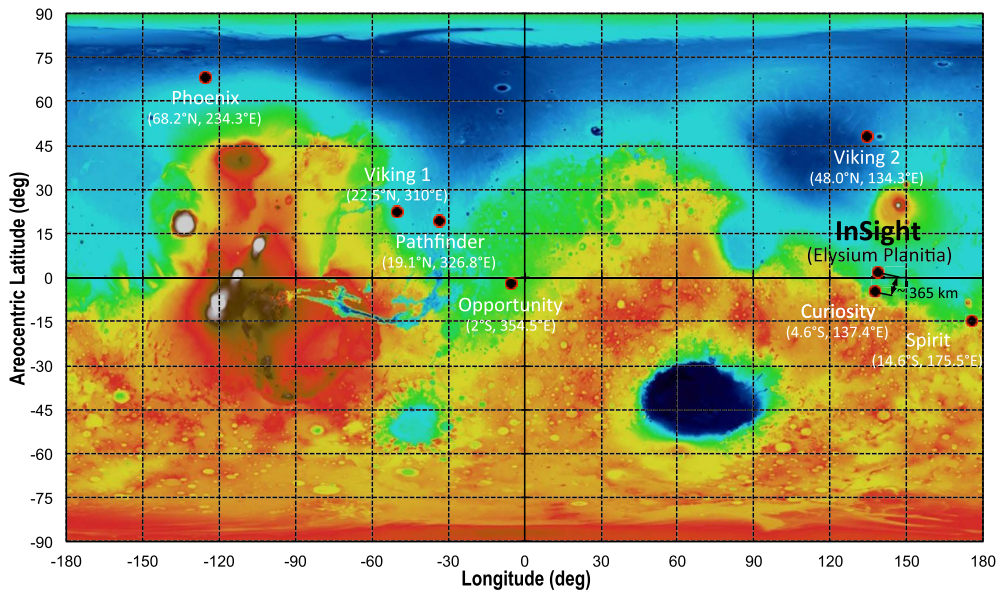


Figure 2. InSight's Target: Elysium Planitia

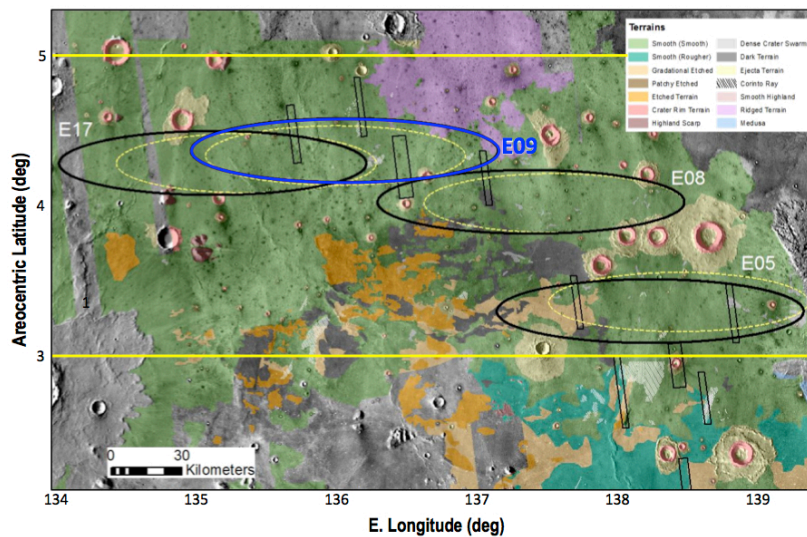


Figure 3. Final Four Candidate Landing Sites

Surface

Once safely on the surface of Mars, the lander is configured for surface operations, solar arrays are deployed, and Science and Engineering data acquired during EDL and during the first hour on the surface will be transmitted to Earth via the lander-to-orbit UHF relay link to assess the state of the lander and to ensure that it has achieved a power/thermal safe state. For the first several sols on the surface, the lander and its surrounding environment, including the workspace, are characterized, the payload elements are checked out, weekly RISE measurements are acquired, and critical data collected on Sol 0 (the landing sol) continue to be relayed back to Earth. After the Science team has selected suitable deployment sites within the workspace, the Instrument Deployment Arm (IDA), places the SEIS and HP³ instruments on the Martian surface. Science monitoring begins once both instruments are on the Martian surface, and SEIS is collecting science data. During this phase, the HP³ mole is released and is allowed to penetrate the Martian regolith until it reaches its final depth over the course of about 30 sols. SEIS and HP³ acquire science data throughout this phase, and RISE measurements are acquired three times per week. The Science Monitoring phase is scheduled for one Mars year, with the possibility of extended surface operations continuing for as long as there is adequate power.

SPACECRAFT

The InSight spacecraft is designed around a core lander that controls all functions throughout all mission phases. Three secondary flight elements (the cruise stage, heatshield, and backshell) provide the additional functions needed for Cruise and EDL. The InSight flight system is almost entirely a re-flight of the Phoenix spacecraft which in turn was an adaptation of the MPL spacecraft design. While InSight takes advantage of the heritage, updates have been made to the design to accommodate the InSight payload, the longer timeline, and changes required due to obsolescence. Figure 4 shows an expanded view of the InSight flight system.

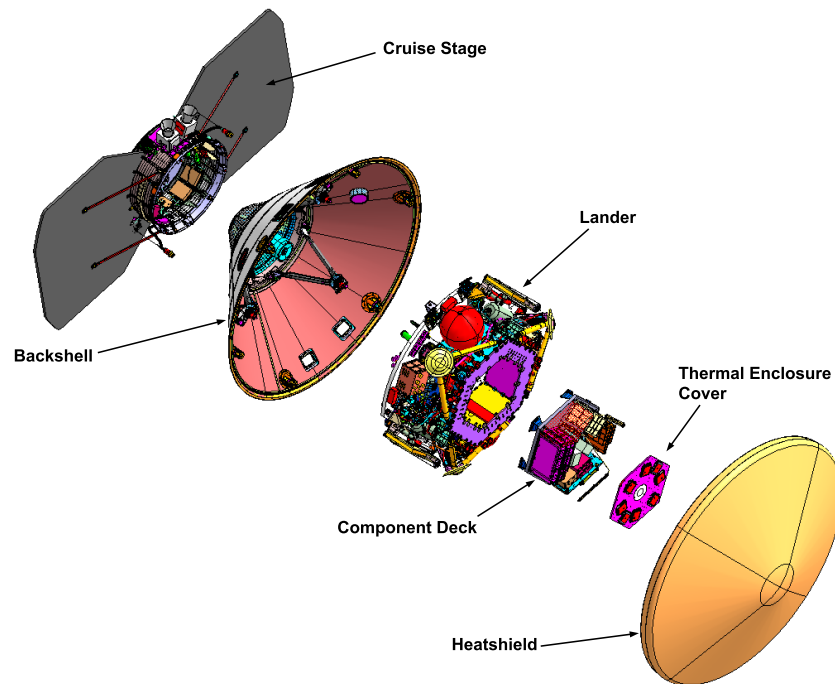


Figure 4. InSight Flight System Expanded View

Attitude Control System

The spacecraft Attitude Control System (ACS) consists of two star trackers, a Mini Inertial Measurement Unit (MIMU), and Sun sensors. The primary attitude determination is done via the star trackers and IMU system. The analog Sun sensors serve as a backup system. Unlike MSL (Mars Science Laboratory) spinning-stabilized attitude control strategy, the InSight spacecraft is three-axis stabilized via an unbalanced thruster control system. The attitude control will be mainly performed by four 1-lbf RCS

thrusters (~4.5 N). The RCS thrusters are fired intermittently to maintain a pre-determined deadband attitude profile. In addition, the 1-lbf thrusters are used to maintain attitude during TCMs (roll only) and safe-mode (3-axis control). The TCM ΔV and pitch/yaw control are performed by four 5-lbf thrusters (~22 N).

Cruise Attitude Profile

The communications antennas (i.e. LGA and MGA) and the solar panels on the InSight spacecraft cruise stage are generally oriented along the spacecraft $-X$ -axis. The cruise attitude strategy is to maintain the $-X$ -axis pointed between the direction to the Earth and direction to the Sun to satisfy telecom and power constraints while meeting thermal and star tracking pointing requirements. This strategy allows a telecom link to Earth using the LGA or MGA antenna and provides sufficient power for spacecraft operations. The cruise phase for InSight is divided into two, early cruise and late cruise, separated by the time the spacecraft reaches a distance of at least 1.084 AU from the Sun. This transition between the early and late cruise phases is planned for May 12, 2016 (Entry – 139 days). In early cruise, the LGA is used and the spacecraft attitude is such that the $-X$ -axis face of the solar arrays are offset 50° from the Sun. This is driven by spacecraft thermal constraints. The Sun off-point direction is measured from the solar array normal and aligned with a vector of $[-0.64278, -0.76604, 0]$. During the early cruise, the ACS and NAV teams will also perform active and passive thruster calibration campaign during this phase. During the late cruise phase, communications are switched to the MGA and the spacecraft $-X$ -axis is pointed in the direction of the Sun, with a vector of $[-1, 0, 0]$. This configuration puts the MGA in the Sun/Earth plane. For the preliminary covariance analysis included in this paper, it is assumed that the transition between the early and late cruise phases occurs when the spacecraft reaches a Sun distance of 1.144 AU (Launch plus 70 days), and the Sun off-point direction during early cruise is aligned with a vector of $[-0.60529, -0.79600, 0]$, i.e., the angle between the $-X$ -axis and the Sun vector is 52.75° .

Attitude Deadbanding

Since the InSight spacecraft is three-axis stabilized, its attitude is not fixed. The attitude will vary within a set of deadbanding constraints defined by spacecraft telecom, power and thermal subsystems. AACS will command the thrusters to fire each time the attitude reaches one side of the deadband. The deadbanding strategy varies during cruise based on the constraints, the Sun-Earth-probe (SEP) angle, and the spacecraft range to the Sun and Earth. The tighter the deadbands, the more thrusting is needed to keep the attitude inside the constraints, which imparts more ΔV and uncertainty into the trajectory. The preliminary GN&C attitude deadbanding strategy is to use 10 degree deadbands on the X and Y axes, and 7.5 deg on the Z axis, ($10^\circ X$, $10^\circ Y$, $7.5^\circ Z$), until Entry – 139 days and then 4 degrees deadbands, ($4^\circ X$, $4^\circ Y$, $4^\circ Z$), for the remainder of the Cruise phase (including the Approach phase). While the deadband ΔV biases are a function of the deadbands, the uncertainties considered in the covariance study are based on the late cruise Phoenix deadband results, that is ($10^\circ X$, $2^\circ Y$, $2^\circ Z$). Since the covariance analysis uses a tighter deadband along the Z-axis (which has the largest contribution to the EFPA) than the preliminary attitude deadbanding strategy, the OD statistics shown in this document might be slightly conservative. It is important to model the ΔV imparted to the system in the OD process in order to meet the delivery accuracy requirements for atmospheric entry. For this reason the flight system records a telemetry packet with thruster information every time a thruster pulse is fired. That telemetry is downlinked and transformed into a text file known as the Small Force File (SFF), which is directly input into the OD and trajectory propagation process. The SFF contains information such as pulse time, pulse length, thruster number, estimated ΔV , and attitude at the time of the pulse⁴.

Cruise Stage Propulsion System

The InSight structure and propulsion systems will be identical to Phoenix with modifications to support the updated avionics hardware and payloads. The Lander propulsion system performs all cruise and EDL propulsion functions. Rocket Engine Modules (REMs) are scarfed through the aeroshell to allow RCS and cruise TCM functions. Specifically, the system consists of four 1-lbf (4.4-N) RCS thrusters to provide attitude control, four 5-lbf (22 N) TCM thrusters to provide ΔV maneuvers during cruise, and twelve 68-lbf (302-N) descent engines to allow for EDL deceleration and attitude control. This configuration, including scarf and REM seal designs, was proven through extensive testing and the Phoenix flight. Figure 5 shows the flight system in cruise configuration.

Telecom System

The cruise telecommunications subsystem comprises fully redundant X-band Small Deep-Space Transponders (SDSTs) and Solid-State Power Amplifiers (SSPAs). It provides redundant transmit and receive capability through a fixed, dual-frequency, medium-gain horn and two low-gain patch antennas (one transmit, one receive). Maximum X-band downlink is 2100 bps (10 bps minimum). Uplink rates range from 7.8125 to 2,000 bps. To accommodate RISE radio science, one of the SDSTs was moved from the Cruise Stage to the Lander and an SSPA was added, both inside the thermal enclosure. Two fixed MGAs provide the signal for RISE with redundancy during landed operations. During EDL, a UHF transceiver relays critical-event data to MRO and back to Earth. A wrap-around antenna on the backshell provides coverage during EDL, followed by use of a monopole antenna during terminal descent. During landed operations, the UHF transceiver performs relay operations to Mars orbiting assets from the Lander twice per day on average. The monopole and helix antennas are functionally redundant¹.

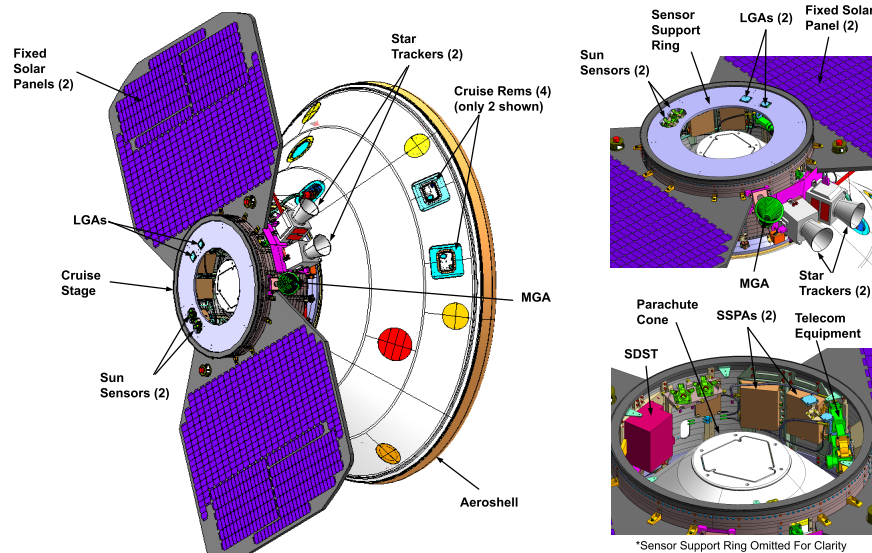


Figure 5. InSight Flight System Cruise Configuration

KEY AND DRIVING REQUIREMENTS

The key driving requirements for mission and navigation design are the following:

The launch/arrival strategy shall...

Launch/Arrival Strategy and EDL Coverage

- ... support a total launch mass of less than or equal to 727 kg.
- ... be compatible with either the Atlas V or Falcon 9 v1.1 launch vehicle as selected through the NASA LSTO process.
- ... be capable of supporting a launch from either the ETR or WTR.
- ... launch between the dates of March 4 and March 26, 2016 both inclusive.
- ... have a launch window duration of at least 30 min.
- ... support at least two launch attempts per day.
- ... support a Mars arrival of September 28, 2016.
- ... approach EDL with a V-infinity upper limit of 3.941 km/s.
- ... land in a region bounded by 5°N to 2°S.

EDL Communications

- ... design a spacecraft trajectory that provides line of sight to the Earth from cruise stage separation to touchdown plus 60 s.
- ... design a spacecraft trajectory that has the capability to support UHF-band telecommunications with the Mars Reconnaissance Orbiter (MRO) from Entry through touchdown plus 60 s.

TCM ΔV and Propellant

- ... ensure 99% probability of successful targeting of the atmospheric entry point within the cruise propellant.
- ... ensure a greater than or equal to 99% probability of performing the mission within the combined Cruise and EDL budgets.
- ... assume that the cumulative ΔV_{99} for all Trajectory Correction Maneuvers (TCMs) targeted to the nominal landing site shall not exceed 30 m/s.

Atmospheric Entry Delivery/Knowledge Accuracies

- The entry vehicle shall approach EDL with an Entry Flight Path Angle (EFPA) of $-12.5 \text{ deg} \pm 0.26 \text{ deg}$, 3-sigma.
- MDNAV shall provide a final update to the entry state (known as the knowledge state) with a 3-sigma Entry Flight Path Angle uncertainty of $\pm 0.15 \text{ deg}$ and a 3-sigma entry time uncertainty of $\pm 0.15 \text{ s}$ not later than the last TCM plus 3 hours.

Planetary Protection

- The injection aimpoint for launch shall be biased away from Mars such that the probability of the launch vehicle upper stage impacting Mars is less than 1.0×10^{-4} for fifty years after launch.
- The probability of non-nominal impact of Mars due to failure during the cruise phase shall not exceed 1.0×10^{-2} .

MISSION DESIGN

Launch/Arrival Strategy

The InSight launch/arrival strategy was designed to provide critical EDL communications via direct-to-Earth and the Mars Reconnaissance Orbiter (MRO) using the UHF link for landing sites between 5°N and 2°S ; this range, encompassed the latitudes of the original set of candidate landing sites. In order to maintain both UHF communications via the MRO and the direct-to-Earth paths, MRO will move its LMST node from its nominal 3 PM to 2:30 PM. The launch period open was constrained to a date not earlier than 03/04/2016 to preserve pre-launch development schedule margin. The close of the launch period is bounded by MRO coverage. Figure 6 shows the InSight Launch/Arrival strategy

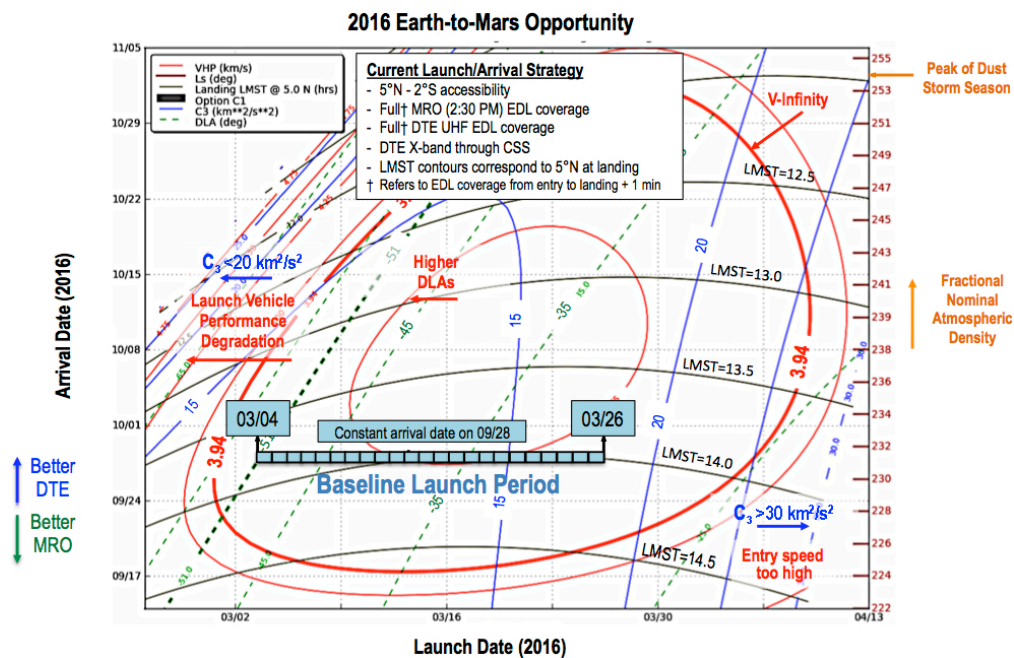


Figure 6. InSight Launch/Arrival Strategy

Launch Period Characteristics

The launch vehicle targets represent the conditions of the osculating departure at the Target Interface Point (TIP) expressed in an Earth-center, inertial, Earth Mean Equator and Equinox of J2000 (EME2000) coordinate system. These Earth-relative target conditions are defined to occur 431 seconds after spacecraft separation from the upper stage of the launch vehicle and are shown in Table 1. The maximum C3 occurs at the close of the launch period, whereas the maximum DLA occurs at the open of the launch period. Assuming a spacecraft launch wet Maximum Possible Value (MPV) mass of 727.0 kg and based on the Atlas V 401 NLS-II contract data, the payload margins for the lowest performance day are over 1,000 kg. Note that the actual performance of these launch vehicles may change due to uncertainties in launch vehicle capabilities and evolution of vehicle designs. Launches from CCAFS assume a 51 deg park orbit inclination whereas launches from VAFB would use a park orbit inclination of 63 deg in order to achieve the desired launch targets while satisfying range constraints from either coast². In order to minimize the time from launch to eclipse exit or spacecraft separation (whichever is later), launching into higher park orbit inclinations is also being considered.

Launch Day	Launch Date (2016)	Arrival Date (2016)	EME2000 Coordinates at TIP (T = minutes from optimal launch time)								
			C3 (km ² /s ²)			DLA (deg)			RLA (deg)		
			Open (T=-60)	Optimal (T=0)	Close (T=+60)	Open (T=-60)	Optimal (T=0)	Close (T=+60)	Open (T=-60)	Optimal (T=0)	Close (T=+60)
1	03/04	09/28	12.059	12.046	12.037	-51.268	-51.201	-51.138	192.080	192.124	192.166
2	03/05	09/28	11.944	11.934	11.928	-49.800	-49.735	-49.674	192.809	192.848	192.884
3	03/06	09/28	11.881	11.873	11.870	-48.367	-48.304	-48.245	193.464	193.499	193.531
4	03/07	09/28	11.866	11.860	11.861	-46.971	-46.911	-46.854	194.062	194.094	194.122
5	03/08	09/28	11.897	11.893	11.897	-45.616	-45.558	-45.503	194.616	194.647	194.671
6	03/09	09/28	11.971	11.969	11.975	-44.305	-44.250	-44.197	195.140	195.168	195.190
7	03/10	09/28	12.085	12.084	12.092	-43.042	-42.989	-42.939	195.641	195.668	195.688
8	03/11	09/28	12.236	12.236	12.247	-41.830	-41.780	-41.732	196.127	196.153	196.171
9	03/12	09/28	12.420	12.423	12.435	-40.672	-40.625	-40.579	196.602	196.627	196.644
10	03/13	09/28	12.636	12.640	12.654	-39.569	-39.525	-39.481	197.068	197.091	197.107
11	03/14	09/28	12.881	12.886	12.902	-38.522	-38.480	-38.439	197.524	197.547	197.561
12	03/15	09/28	13.153	13.159	13.177	-37.530	-37.491	-37.451	197.972	197.994	198.008
13	03/16	09/28	13.450	13.456	13.476	-36.590	-36.554	-36.516	198.409	198.431	198.444
14	03/17	09/28	13.770	13.778	13.798	-35.702	-35.668	-35.632	198.837	198.858	198.870
15	03/18	09/28	14.113	14.122	14.144	-34.863	-34.831	-34.798	199.255	199.275	199.287
16	03/19	09/28	14.479	14.489	14.512	-34.072	-34.042	-34.011	199.664	199.683	199.695
17	03/20	09/28	14.867	14.878	14.902	-33.328	-33.300	-33.271	200.062	200.081	200.092
18	03/21	09/28	15.278	15.290	15.315	-32.631	-32.605	-32.578	200.450	200.468	200.478
19	03/22	09/28	15.711	15.724	15.749	-31.985	-31.961	-31.936	200.821	200.838	200.847
20	03/23	09/28	16.164	16.178	16.205	-31.389	-31.367	-31.343	201.158	201.172	201.179
21	03/24	09/28	16.635	16.649	16.676	-30.812	-30.789	-30.763	201.428	201.440	201.444
22	03/25	09/28	17.125	17.141	17.169	-30.184	-30.159	-30.132	201.681	201.695	201.703
23	03/26	09/28	17.648	17.666	17.695	-29.556	-29.532	-29.508	202.015	202.031	202.042

Table 1. Launch Targets

EDL Coverage Characteristics

The selected launch period satisfies the requirement of maintaining full EDL communications from Entry to landing plus 1 min via both MRO and direct-to-Earth. It is assumed that EDL communications are available when the asset (MRO or Earth) has direct line of sight to InSight, i.e., InSight is not occulted by Mars as seen by the asset, and the antenna angle is within the antenna angle constraints. The antenna angle is defined as the angle between the atmosphere-relative anti-velocity vector and the line of sight to the asset. Even though, the resulting PUHF antenna boresight actually points along the $-Z$ -axis, 6-DOF simulations indicate that the anti-velocity vector is a valid approximation to the modeling of the $-Z$ -axis direction

during EDL. The antenna angle constraint is 135 deg. It is also required that the elevation angle from landing to landing plus 1 minute is at least 10 deg above the horizon line. Based on these constraints, a range of MRO mean anomalies at Entry Interface Point (EIP) has been identified. This range defines the orbital phasings from which MRO could provide EDL communication services. Given MRO's on-orbit phasing control of ± 30 s or ± 1.6 deg, only mean anomaly ranges of at least 5 deg are acceptable. This value includes margin to account for evaluation of EDL comm geometries using conic approximations. Figure 7 illustrates the arrival geometry for a launch at the open of the launch period.

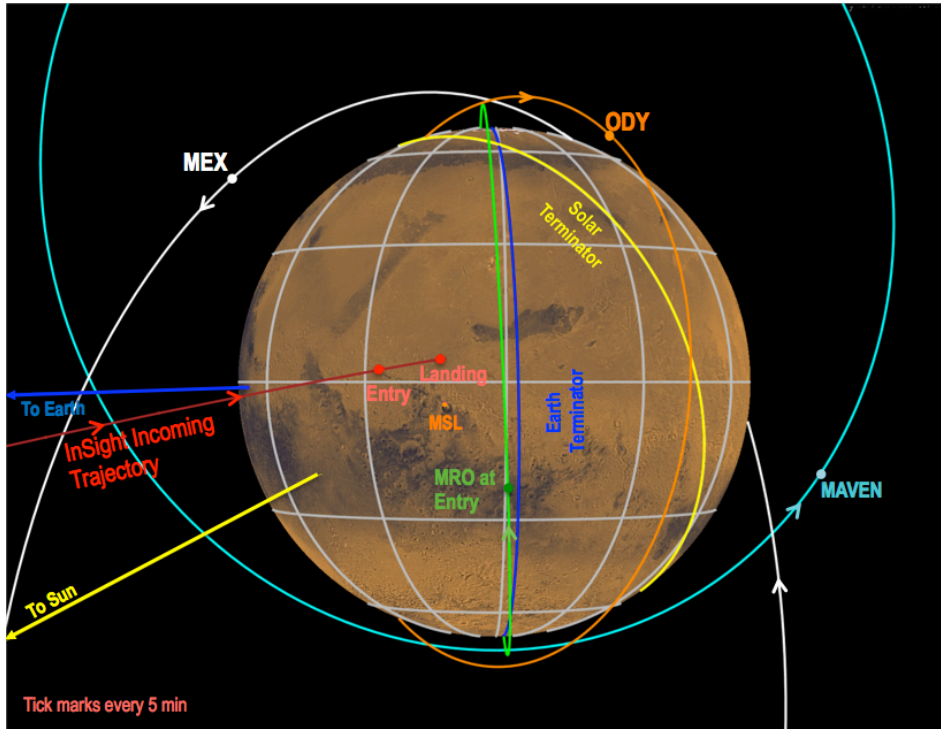


Figure 7. Arrival Geometry (03/04/2016 Launch)

Launch Trajectory Characteristics

Due to the high southerly launch declinations, the InSight interplanetary trajectories limit the Goldstone-Madrid tracking, requiring an alternative Δ DOR baseline such as Madrid-New Norcia or Canberra-Usuda to complement Canberra-Goldstone in order to achieve the 3-sigma EFPA uncertainty requirement of less than ± 0.26 deg. Figure 8 shows the geocentric declination during cruise⁴.

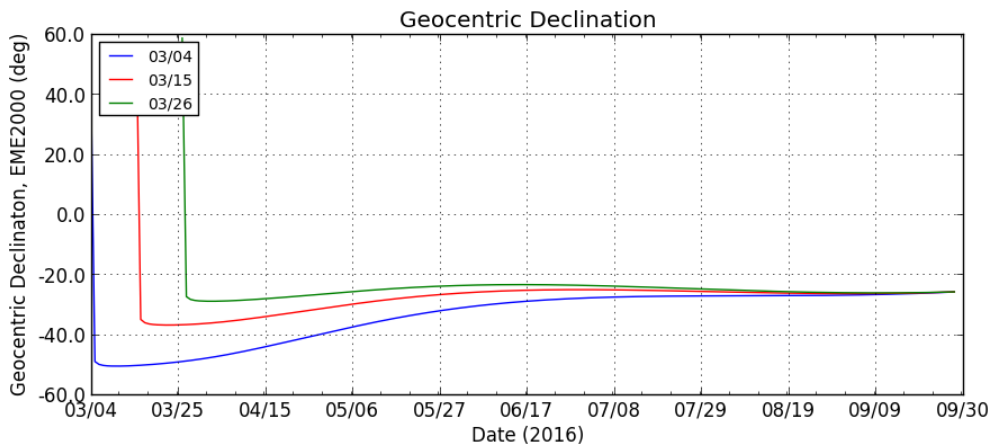


Figure 8. Geocentric Declination during Cruise

NAVIGATION DESIGN

TCM Profile

The launch vehicle will target the spacecraft in a direction that is biased away from the optimal atmospheric entry aimpoint for planetary protection purposes in order to ensure that there is less than a 10^{-4} chance that the upper stage will impact Mars for fifty years. In addition, planetary protection requires that the probability of any anomaly causing impact of the InSight spacecraft with Mars must be less than 10^{-2} (non-nominal impact probability requirement). The injection bias will be vectorially combined with the dispersions from the actual launch vehicle performance to generate the correction necessary to aim the spacecraft at its Mars entry point. Analysis has shown that scheduling six TCMs is adequate to ensure the atmospheric entry aimpoint conditions within the allowable error bounds are met.

Event	Location	OD Data Cutoff	Objectives
TCM-1	L + 10d	TCM – 5d	Removes launch vehicle targeting bias and injection errors, potentially targets to Entry Interface Point (EIP) defined for specific launch date. TCM-1 includes a deterministic component required to remove the launch vehicle aimpoint bias
TCM-2	L + 60d	TCM – 5d	Statistical maneuver to correct for orbit determination errors and TCM-1 execution errors; targets to EIP for specific launch date
TCM-3	E – 45d	TCM – 5d	Statistical maneuver to correct for orbit determination errors and TCM-2 execution errors; targets to EIP for specific launch date
TCM-4	E – 15d	TCM – 1d	Statistical maneuver to correct for orbit determination errors and TCM-3 execution errors; targets to EIP for specific launch date
TCM-5	E – 8d	TCM – 1d	Statistical maneuver to correct for orbit determination errors and TCM-4 execution errors; targets to EIP for specific launch date
TCM-5x	E – 5d	TCM – 1d	Same objectives as TCM-5. Performed only if TCM-5 is not executed nominally
TCM-6	E – 22h	TCM – 10h	Statistical maneuver to correct for orbit determination errors and TCM-5/5x execution errors; targets to EIP for specific launch date
TCM-6x	E – 8h	TCM – 24h	Final opportunity for entry targeting maneuver. Performed only if TCM-6 does not take place. Will be designed at the same time as TCM-6 to define a menu of candidate maneuvers selected to minimize the target miss on the Mars surface.

Table 2. TCM Schedule

Orbit Determination

The baseline radiometric data types used for orbit determination are two-way coherent Doppler, two-way ranging, and Delta Differential One-way Range (Δ DOR) measurements generated by the DSN X-band tracking system. All data types are derived from a coherent radio link between the spacecraft and a receiver at a DSN ground station. In the case of Δ DOR measurement, a radio signal from a quasar will also be used to obtain the measurements. Doppler data yield a measurement of line-of-sight spacecraft range rate. During tracking passes in the two-way coherent mode of operation, the DSN tracking system measures Doppler shift by accumulating the cycles of the downlink carrier signal in order to determine the difference between the transmitted and received frequencies. Two-way range is also a line-of-sight measurement. The DSN ranging system constructs an estimate of the range to the spacecraft by measuring the round-trip light time of a radio signal between the ground station and the spacecraft.

Δ DOR is a Very Long Baseline Interferometry measurement of a spacecraft using pairs of DSN stations (either Goldstone-Madrid or Goldstone-Canberra) and an intergalactic radio source (i.e., quasar). Two DSN stations simultaneously observe the spacecraft followed by simultaneous observations of the quasar. Δ DOR directly measures angular separation between the spacecraft and the quasar in the direction of the projected

baseline between the two stations. The Δ DOR observable is a phase delay time expressed in units of nanoseconds (ns) that is equivalent to an angular separation between the spacecraft and the quasar; a delay of 1 ns corresponds to an angular separation of ~ 37.5 nrad. Δ DOR measurements determine the spacecraft position in the plane of the sky. The Goldstone-Madrid baseline (oriented East- West) primarily measures the right ascension component of the spacecraft position, and the Goldstone-Canberra baseline (oriented Northeast-Southwest) primarily measures the declination component of the spacecraft position, with a substantial dependency on right ascension as well. Δ DOR measurements are generally scheduled with alternating baselines. The Δ DOR data type complements line-of-sight Doppler and range measurements because of its orthogonality to those data types.

Tracking Schedule

The InSight mission will rely on the NASA Deep Space Network (DSN) to provide the tracking resources necessary to achieve the mission objectives. Table 3 shows the DSN tracking schedule used for OD the analyses.

Phase	Relative Dates	Doppler/Range	Δ DOR
Launch	Launch to L + 15 days	Continuous 34-m coverage	None
Cruise	L + 15 days to L + 30 days	Three 34-m 8-hour pass/week*	
	L + 30 days to E - 60 days		One session per week
	E - 60 days to E - 30 days	One 34-m 8-hour pass/day*	Two sessions per week
EDL	E - 30 days to Entry	Continuous 34-m coverage	Two sessions per day. Alternating DSN and ESA/DSN
Surface	Landing to landing + 62 days	One 70-m 3-hr pass/day	None
	Landing + 62 days to EOM	One 34-m 1-hr pass/week	

* Additional 4 days continuous coverage for TCMs

Table 3. DSN Tracking Schedule

OD Filter Assumptions

Orbit determination processing is accomplished with a multiple batch consider-parameter filter, incorporating a baseline dataset consisting of two-way coherent Doppler, two-way coherent ranging data, and Δ DOR measurements. The OD assumptions are shown in Table 4. All TCMs contained within the data arc are estimated. Future TCMs (i.e., with respect to a given data cutoff time) are treated in one of two ways. For generating entry delivery uncertainties, the TCM directly after the data cutoff time is considered in the filter at the a priori uncertainty, while any other future TCMs are ignored. For generating orbit determination covariance matrices for maneuver analyses, all future TCMs are ignored, and maneuver execution errors are modeled in the maneuver analysis process.

Spacecraft AACS Δ Vs (e.g., spacecraft attitude maintenance) are estimated in the OD filter when these events fall within the data arc, and they are considered at all times in the future (i.e., between the end of the data arc and Entry). Δ V from AACS is modeled with two three-component stochastic accelerations with zero mean in the development phase. The first acceleration models the uncertainty associated with short-term randomness of individual thruster firings. The second acceleration models the uncertainty associated with a long-term total thrust offset that tends to bias the trajectory. In operations the Δ V from attitude maintenance will be modeled as discreet impulsive events. The solar pressure model consists of five components representing the solar arrays, the launch vehicle adapter on the cruise stage, the cruise stage outer ring, and the backshell (2 components). For navigation analyses the solar pressure uncertainty is modeled using a three-axis scale factor on the total solar pressure acceleration.

Range data biases, solar pressure acceleration, and attitude maintenance accelerations are estimated stochastically. The data biases are estimated during each tracking pass. Moreover, dynamic model margin has been incorporated to account for non-gravitational acceleration mismodeling. The considered

parameters consist of Earth orientation parameters, media calibrations, quasar locations, station locations, Mars’s GM as well as Earth and Mars ephemerides.

Error Source	Estimate(E), Estimate through Stochastics (S) or Consider (C)	Uncertainties (1-sigma)		
		Baseline	Degraded	No Margin
2-way Doppler weight (mm/s)	-	0.1	0.2	0.05
Range weight (m)	-	3	6	3
DSN ΔDOR weight (ps)	-	60	120	40
ESA ΔDOR weight (ps)	-	120	200	60
DSN ΔDOR latency (hr)	-	2*	6*	2
ESA ΔDOR latency (hr)	-	24*	48*	24
TCM and TCM Slews	E	Gates Model + L2 Slew Requirement	1.2 x Req.	0.8 x Req.
Short Term Deadbanding (X/Y/Z) (km/s ²)	S	2.25e-11 4.5e-12 4.5e-12	1.5 x Baseline	2/3 x Baseline
Long Term Deadbanding (km/s ²)	S	7.4e-12 1.5e-12 1.5e-12	1.5 x Baseline	2/3 x Baseline
Solar Pressure Scale Factor (%)	S	3	10	3
Range Bias (m)	S	2	4	1
Day Ionosphere (cm)	C	55	75	55
Night Ionosphere (cm)	C	15	30	15
Wet Troposphere (cm)	C	1	2	1
Dry Troposphere (cm)	C	1	2	1
X/Y Pole (cm)	C	1	2	1
UT1 (cm)	C	2	4	1
Quasar Locations (nrad)	C	1	2	1
Mars GM (km ³ /s ²)	C	2.8e-4	2.8e-4	2.8e-4
Earth-Mars Ephemeris scale	C	1.0 x	1.5 x	0.5 x

Table 4. Orbit Determination Filter Assumptions

Approach Navigation Accuracies

The combination of orbit determination errors and maneuver execution errors mapped to the atmospheric entry interface point is referred to as the delivery accuracy. TCMs 4, 5, and 6 during the Approach phase are the key maneuvers used to target to the desired entry interface conditions. The entry interface conditions consist of inertial entry flight path angle (EFPA), B-plane angle, and time at the entry interface point, defined as Mars radius equal to 3522.2 km and are illustrated in Figure 9. These conditions can also be met by targeting a B-plane aimpoint (B•T, B•R) along with a time of flight

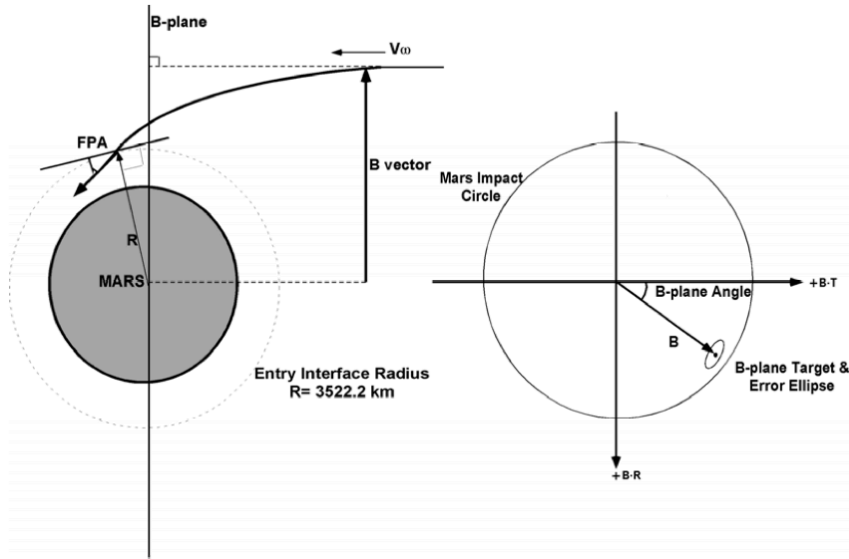


Figure 9. Entry Interface Targets

The entry interface conditions are derived from the desired landing target based on the trajectory of the spacecraft during the EDL phase. Targeting a specific B-plane angle and entry time corresponds to targeting latitude and longitude on the surface. The EFPA is a parameter that affects the ballistic trajectory of the EDL system through the atmosphere. The atmospheric trajectory and therefore EFPA are constrained by the limits of the flight system. The flight system is required to be able to accommodate an inertial EFPA of -12.5 deg and 3σ EFPA dispersions consistent with execution of TCM-6 at Entry -22 hours.

Each TCM has an associated entry uncertainty that is made up of errors in orbit determination and maneuver execution. In order to satisfy the physical constraints of the flight system and to limit the size of the landing error ellipse, the navigation system is required to satisfy the EFPA requirement specified in the entry targeting requirement accuracy requirement. The current EDL baseline is to target an inertial EFPA of -12.5 deg with an uncertainty of ± 0.26 degrees (3σ).

The EFPA error is not only a function of delivery accuracy, but it is also a function of the targeted B-plane angle. The dependence of EFPA error on B-plane angle is due to the projection of the B-plane error ellipse (i.e. delivery accuracy ellipse) onto the EFPA direction. This relationship is shown in Figure 10.

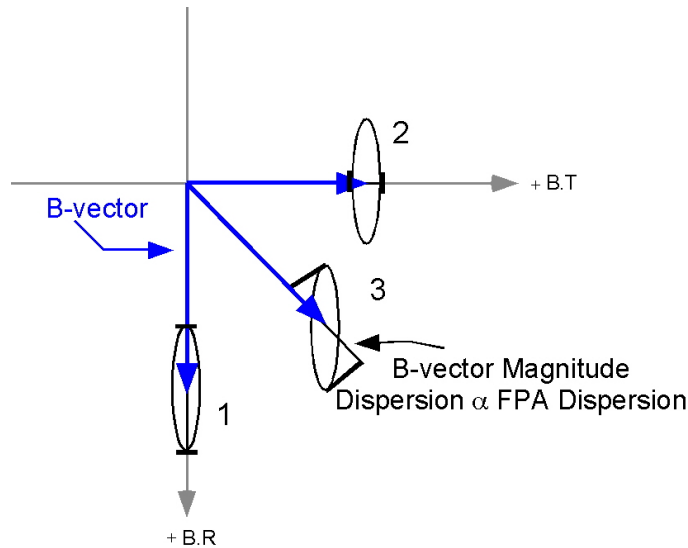


Figure 10. Dependence of EFPA Error on B-plane Angle

The EFPA for a given trajectory is a function of the magnitude of the B-vector or impact parameter. If the semi-major axis of the B-plane error ellipse lies along the B-vector (Ellipse #1 in Figure 10), then the

maximum component of the error lies in the EFPA direction and the EFPA uncertainty is maximized. If the semi-minor axis of the B-plane error ellipse lies along the B-vector (Ellipse #2 in Figure 10), then the minimum error component lies in the EFPA direction and the EFPA uncertainty is minimized. Ellipse #3 in Figure 10 illustrates an intermediate case. In general, the EFPA uncertainty is a function of B-plane angle and B-plane error ellipse orientation. However, for a given trajectory and set of orbit determination assumptions, such as data types used, the error ellipse orientation remains reasonably constant for all B-plane angles.

Approach Delivery

The InSight delivery accuracy results from TCM-6 are given in Table 5. This table shows the variation in EFPA uncertainty for open, middle and close of the launch period. B-plane error ellipses resulting from the TCM-5 delivery, TCM-6 delivery and the corresponding knowledge statistics for the worst EFPA uncertainty day (middle of the launch period) targeted to the reference E9 landing site are shown in Figure 11. The results show that the entry knowledge requirement can be easily met at the E-6 hours OD cutoff. Note the InSight B-plane error ellipse is nearly circular due to the dominance of the slew errors. A nearly circular B-plane error ellipse minimizes the B-plane angle’s effect on the EFPA dispersion.

Date (2016)	EFPA Uncertainty (3σ , deg)
03/04	0.210
03/16	0.212
03/26	0.205

Table 5. TCM-6 EFPA Delivery 3σ Uncertainty

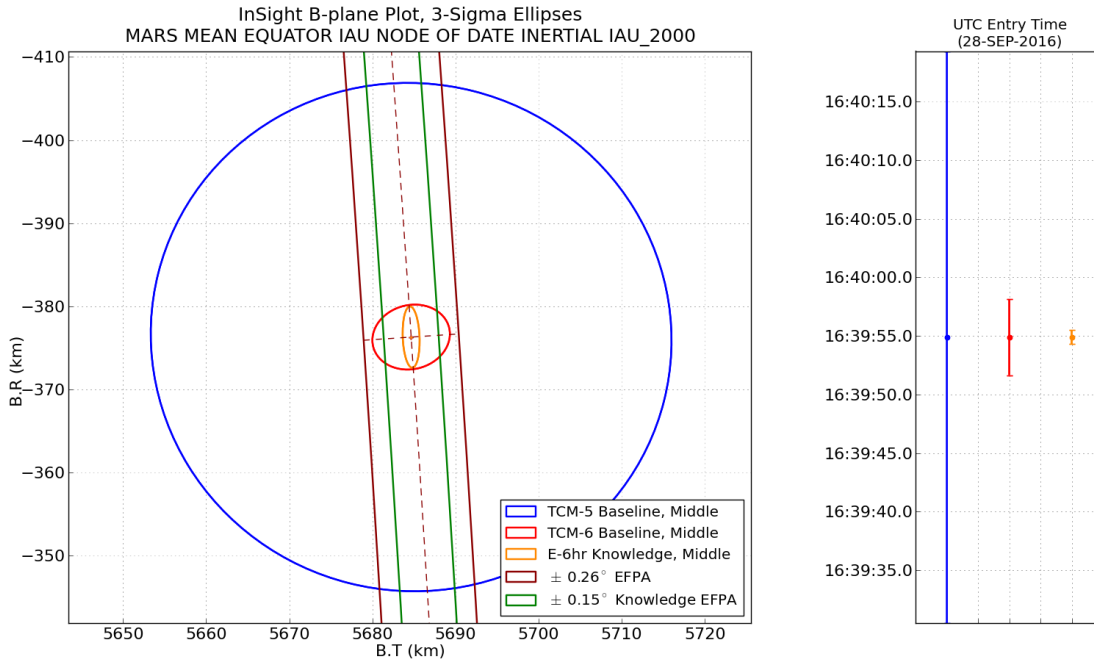


Figure 11. Approach B-Plane

Sensitivity Analysis

The “No Margin” case represents an optimistic scenario for which the following assumptions hold: (1) unlikely (but possible) faults and/or out-of-spec performance (both of which have been accounted for in setting error levels) do not occur, (2) all requested Doppler and range tracking passes are successful, and (3) all requested Δ DOR measurements are successful. The difference in results between the “No Margin”

and the baseline cases quantifies the amount of margin included in the navigation design. The assumptions for the sensitivity cases and the “No Margin” case are given in Table 4. The table includes the nominal assumptions labeled as “Baseline”, a degraded uncertainty for each parameter studied labeled as “Degradation” and an improvement over the baseline for each parameter studied labeled as “No Margin”. All the “No Margin” improvements make up the “No Margin” cases. Figure 12 illustrates the history mapping of these three filter scenarios. As seen from the figure, both “Baseline” and “No Margin” cases easily satisfy the EFPA requirement. The “Degraded” case exceeds the requirements by about 40%. As shown in this Figure, the EFPA uncertainties will not meet the requirement until a couple days before the TCM-6 data cutoff. Figure 13 shows the associated B-plane error ellipses with respect to the Entry requirements. Figure 14 shows the Δ DOR sensitivity to different combinations of NASA, ESA, and JAXA baselines during the last two weeks prior to EDL⁴.

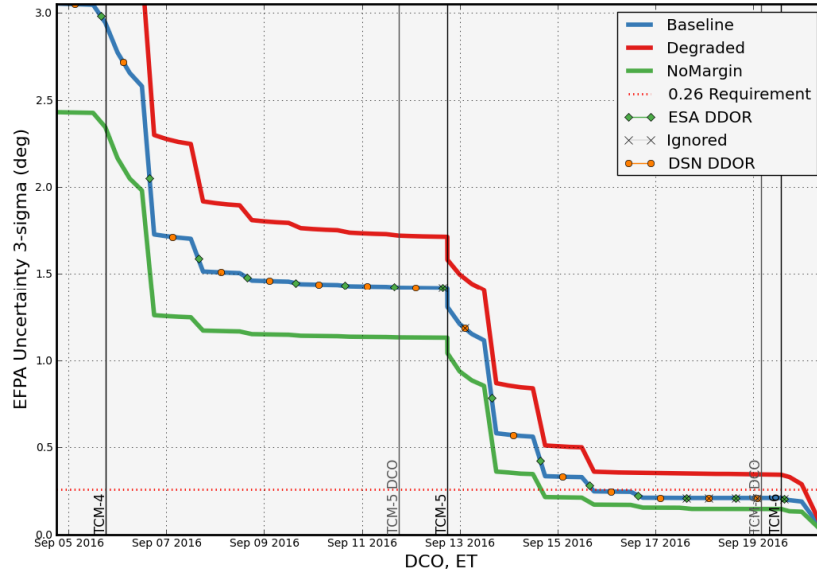


Figure 12. EFPA Uncertainty Evolution (Baseline/No Margin/Degraded)

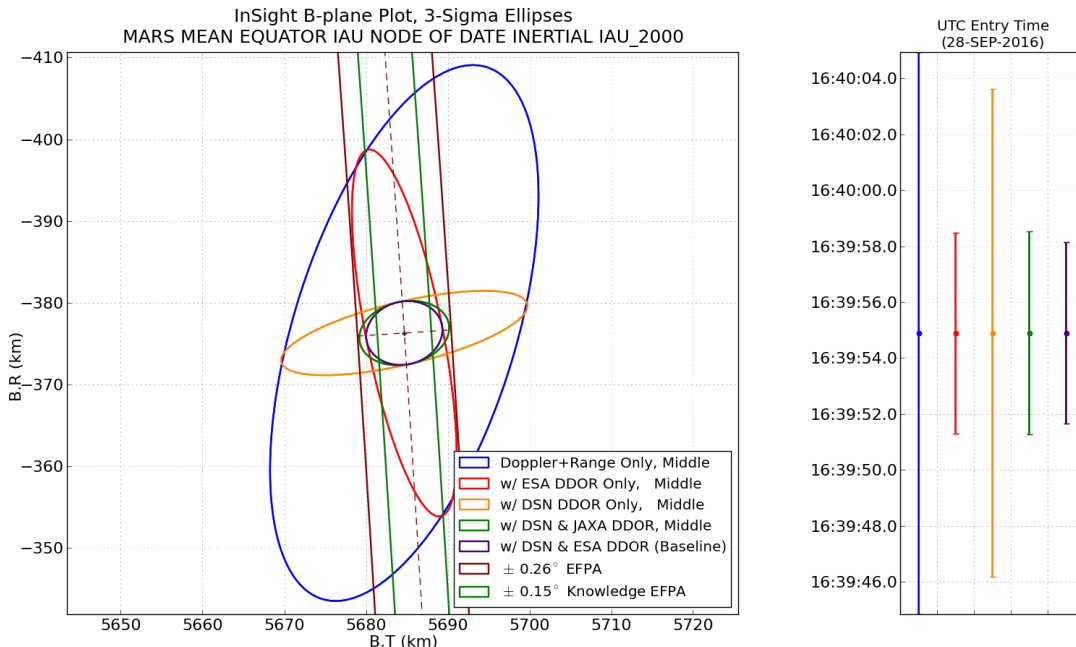


Figure 13. Approach B-Plane (Δ DOR Sensitivity)

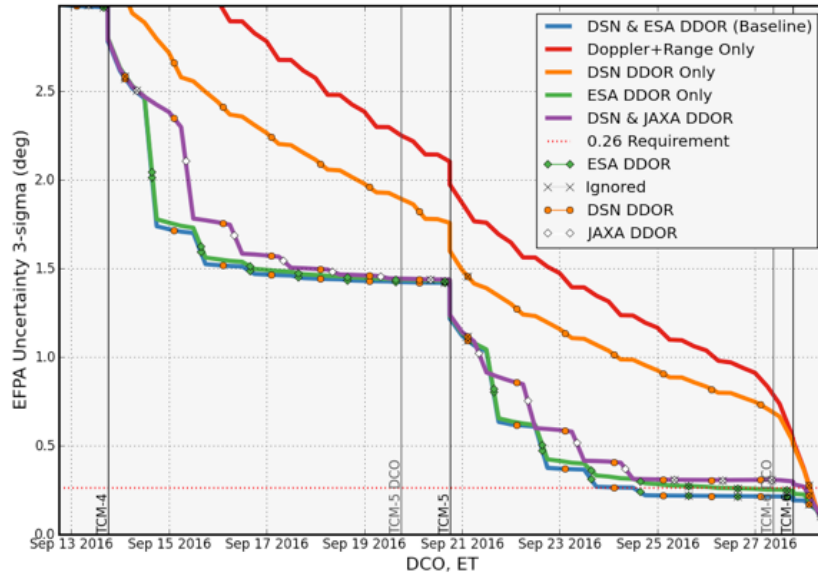


Figure 14. EFPA Uncertainty Evolution (Δ DOR Sensitivity)

Propulsive Maneuver Analysis

A series of six trajectory correction maneuvers (TCMs) are planned during the Cruise phase as shown in Table 2. The locations of the TCMs were selected based on the following drivers: (1) Provide sufficient time between Launch and TCM-1 for spacecraft checkout and design of TCM-1, (2) provide sufficient time between TCMs to allow for TCM reconstruction, orbit determination, and sequence generation for the upcoming TCMs, minimize Mars atmospheric entry delivery errors, (4) minimize total mission propellant usage consistent with entry mass requirements, and (5) minimize operational complexity.

Maneuver Execution Error Models

The accuracy with which each TCM can be executed is a function of the propulsion system behavior and the attitude control system, which maintains the pointing of the spacecraft during thruster firings. Maneuver execution errors are described in terms of components that are proportional to the commanded ΔV magnitude, and components that are independent of ΔV magnitude. The 3σ execution errors listed in Table 6 are the same for all TCM ΔV magnitudes, except for the proportional pointing errors.

ΔV Magnitude		Fixed Magnitude Error	Proportional Magnitude Error	Fixed Pointing Error	Proportional Pointing Error, Total
Min	Max				
m/s	m/s	m/s	%	m/s per axis	%
0.04	0.3	0.02	2	0.003	2
0.3	1.5	0.02	2	0.003	$(8/1.2)* \Delta V $
1.5	5	0.02	2	0.003	10
5	20	-	2	0.003	$(-8/15)* \Delta V +12.667$
20		-	2	0.003	2

Table 6. Maneuver Execution Errors

These errors assume that the TCM thrusters are already aligned with the required ΔV direction, so attitude slews to and from the burn attitude, and the related errors, are not included in these error estimates. In addition, both the fixed and proportional pointing errors are defined as per axis values that apply equally

to both spacecraft body axes normal to the thrust direction. As such, these are circular pointing errors consistent with the Gates simplified maneuver execution error model. Modeling non-circular pointing error adds complexity requiring knowledge of the roll attitude about the thrust direction. Instead, conservative estimates of per axis pointing uncertainties are applied as circular pointing errors.

For InSight, attitude slews to and from the TCM burn attitude are implemented with RCS thrusters. Each RCS thruster has a component of thrust in all three spacecraft body axes. Thrust in the Y- and Z- directions are nominally balanced, but not in the +X direction. As a result, each time an RCS thruster is fired there is a ΔV imparted along the spacecraft +X direction.

Slew errors are non-burn ΔV event uncertainties that are independent of the TCM ΔV magnitude, and as such are treated as fixed error sources. As shown in Table 7, these include slew errors to and from the TCM burn attitude, and errors that arise from pre- and post-burn inertial hold and TCM rate damping sources. Errors along the X-axis contribute to fixed ΔV magnitude errors, while errors along the Y- and Z- axes introduce fixed pointing errors. As defined in Table 6, these errors have been mapped to the TCM burn attitude. Because these fixed errors are independent, they have been combined by RSS on each body axis. These values are consistent with observed Phoenix performance and considered appropriate for Phase B analysis pending verification by InSight GNC error analyses during Phase C. To protect against possible growth in the non-burn ΔV uncertainties, InSight Navigation has added a 20% design margin.

Non-Burn ΔV Event Uncertainties [TBR]	Spacecraft Body Frame		
	S/C X (m/s)	S/C Y (m/s)	S/C Z (m/s)
Slew To & From ΔV Attitude	0.0154	0.0116	0.0183
Pre & Post-Burn Inertial Hold & TCM Rate Damp	0.0092	0.0387	0.0080
Combined Slew Errors	0.0180	0.0416	0.0200
Combined Slew Errors with 20% Design Margin	0.0216	0.0500	0.0240

Table 7. Non-burn ΔV Uncertainties

The TCM burn errors in Table 6 and the non-burn slew errors from Table 7 are combined to define total errors consistent with the Gates error model formulation. Here, only the fixed errors are affected, as slew errors do not affect proportional ΔV errors. The total 3σ fixed pointing uncertainty is dominated by slew errors in the s/c Y-axis (0.05 m/s), so the total 1σ value listed in Table 8 is 0.01666 m/s per axis. The combined fixed magnitude error is the RSS of 0.02 m/s and the spacecraft X-axis component of the non-burn error of 0.0216 m/s for a resulting 1σ value of 0.00982 m/s. Note that pointing errors remain the only error source that varies with TCM ΔV magnitude⁴.

ΔV Magnitude	Fixed Magnitude Error	Proportional Magnitude Error	Fixed Pointing Error	Proportional Pointing Error
m/s	m/s	unitless	m/s per axis	rad per axis
0.04	0.00982	0.00667	0.01666	0.00472
0.3	0.00982	0.00667	0.01666	0.00472
1.5	0.00982	0.00667	0.01666	0.02357
5	0.00982	0.00667	0.01666	0.02357
20	0.00982	0.00667	0.01666	0.00472
>>20	0.00982	0.00667	0.01666	0.00472

Table 8. Combined Burn and Non-Burn Maneuver Execution Errors

TCM ΔV and Propellant Statistics

Using preliminary Injection Covariance Matrices (ICMs) provided by ULA that define predicted launch vehicle injection errors, Mission ΔV requirements for the planned TCM schedule were estimated for each

launch date by performing 5000-sample Monte Carlo linear error analyses that model errors due to launch vehicle injection, orbit determination, and maneuver execution. These errors are consistent with the turn-burn-turn execution errors described earlier. Table 9 shows the TCM ΔV statistics for the worst ΔV_{99} day (middle of launch period).

Event	TCM Schedule		TCM ΔV Statistics (m/s)					Cumulative ΔV_{99}
	Relative Time	OD Data Cutoff	Deterministic ΔV	FOM	Mean ΔV	1σ ΔV	ΔV_{99}	
TCM-1	L+10d	TCM-5d	2.982	4.103	4.742	1.777	10.468	10.468
TCM-2	L+60d	TCM-5d			0.224	0.154	0.775	10.876
TCM-3	E-45d	TCM-5d			0.112	0.054	0.276	10.977
TCM-4	E-15d	TCM-1d			0.084	0.035	0.182	11.071
TCM-5	E-8d	TCM-1d			0.051	0.020	0.106	11.149
TCM-5*	E-5d	TCM-1d						
TCM-6	E-22h	TCM-10h			0.203	0.092	0.452	11.375
TCM-6*	E-8h	TCM-24h						
		Total ΔV:	2.982	4.103	5.416	1.850	11.375	

* Contingency maneuvers

Table 9. TCM ΔV Statistics

Injection Aimpoint Biasing

All trajectories contain launch biases such that the deterministic component of TCM-1 is minimized while the probability of the launch vehicle upper stage impacting Mars remains at least 0.6×10^{-4} at the first encounter. In order to satisfy the 1.0×10^{-4} planetary protection requirement for 50 years, injection biasing strategies have been identified which bias further away the injection aimpoint at a low deterministic TCM-1 ΔV cost of ~ 1 m/s.

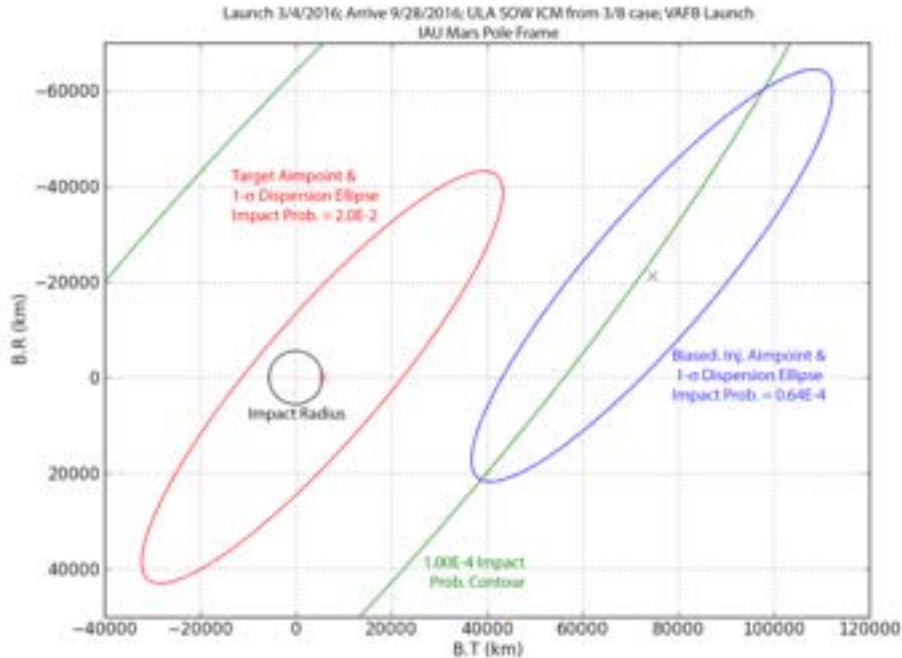


Figure 15. Biased Injection Aimpoint (03/04/2016)

Non-nominal Impact Probability

Additionally, planetary protection requirements state that the probability of non-nominal impact of Mars due to failure during the Cruise Phase shall not exceed 1.0×10^{-2} . A non-nominal impact is defined as an impact that could result in the break-up of the spacecraft and release of terrestrial contaminants on Mars. Overall, non-nominal impact probability is the cumulative sum of the probability of non-nominal impact following each TCM. The probability of non-nominal impact for TCMs 1 through 5 is defined as the probability of impact after each TCM multiplied by the probability that the following maneuver does not occur. The total non-nominal impact probability is computed as:

$$\sum_{i=1}^n P(i)Q(i+1) \leq 10^{-2}$$

where $P(i)$ is the probability of impact after each TCM, and $Q(i+1)$ is the probability that the next maneuver does not occur. Table 10 shows the cumulative non-nominal impact probability for the open, middle, and close of the launch period. For each launch date, TCMs 1, 2, and 3 are the major contributors to non-nominal impact probability, driven by the large time between TCMs early in the mission and that $Q(i+1)$ is defined directly by a spacecraft failure rate of 7×10^{-5} /day. The cumulative probability of non-nominal impact for each launch date satisfies the requirement of 1.0×10^{-2} .

Event	Location	Open (March 4, 2016)			Middle (March 16, 2016)			Close (March 26, 2016)		
		P(i)	Q(i+1)	P(i)*Q(i+1)	P(i)	Q(i+1)	P(i)*Q(i+1)	P(i)	Q(i+1)	P(i)*Q(i+1)
Launch		0	9.768E-7	0.000E+0	0	9.768E-7	0.000E+0	0	9.768E-7	0.000E+0
Injection		6.36E-5	7.021E-4	4.464E-8	5.40E-5	7.021E-4	3.788E-8	5.58E-5	7.021E-4	3.920E-8
TCM-1	L+10d	0.486	3.511E-3	1.705E-3	0.491	3.511E-3	1.722E-3	0.489	3.511E-3	1.717E-3
TCM-2	L+60d	0.485	7.205E-3	3.494E-3	0.488	6.368E-3	3.108E-3	0.488	5.669E-3	2.764E-3
TCM-3	E-45d	0.466	2.092E-3	9.749E-4	0.473	2.093E-3	9.904E-4	0.470	2.094E-3	9.837E-4
TCM-4	E-15d	0.376	4.877E-4	1.832E-4	0.404	4.880E-4	1.973E-4	0.394	4.882E-4	1.922E-4
TCM-5	E-8d	0.276	4.933E-4	1.362E-4	0.325	4.936E-4	1.605E-4	0.306	4.939E-4	1.510E-4
TCM-6	E-22h	1.00	6.383E-5	6.383E-5	1.00	6.387E-5	6.385E-5	1.00	6.390E-5	6.389E-5
			Total	6.56E-3		Total	6.24E-3		Total	5.87E-3

P(i) : probability of impact after maneuver i
 = total impact probability (100 km atmosphere) for all maneuvers except TCM-6
 = probability of impact for non-nominal entry flight path angles for TCM-6
 Q(i+1) : probability of not being able to execute maneuver i+1 given that maneuver i has occurred.

Table 10. Probability of Non-Impact

ENTRY, DESCENT, AND LANDING

The basic elements of the InSight EDL system remain unchanged from Mars Phoenix. As shown in Figure 16, the spacecraft arrives at Mars in the Pre-Entry Configuration, which consists of a cruise stage and entry vehicle. The cruise stage, which provides solar power and navigation functions during the cruise to Mars, is jettisoned prior to atmospheric entry, leaving the Entry Configuration. More than 99% of the Mars relative energy possessed by the vehicle is removed via entry configuration atmospheric drag during hypersonic and supersonic flight. At target deploy conditions, a Viking heritage disk-gap-band (DGB) supersonic parachute is deployed. This parachute configuration further reduces the energy of the EDL system, while carrying out key activities in preparation for terminal descent. These activities include jettison of the entry vehicle heatshield exposing the lander inside the entry vehicle. Heatshield jettison is followed by lander leg deploy and radar power on. The radar is used for both altimetry and velocimetry and is a key element of the landing system. Upon reaching a desired velocity/altitude state, the lander separates from the parachute/backshell and begins using a system of 12 pulsed thrusters to perform a gravity turn powered descent. Touchdown and engine cutoff occurs when one of three landing legs contacts the ground⁵.

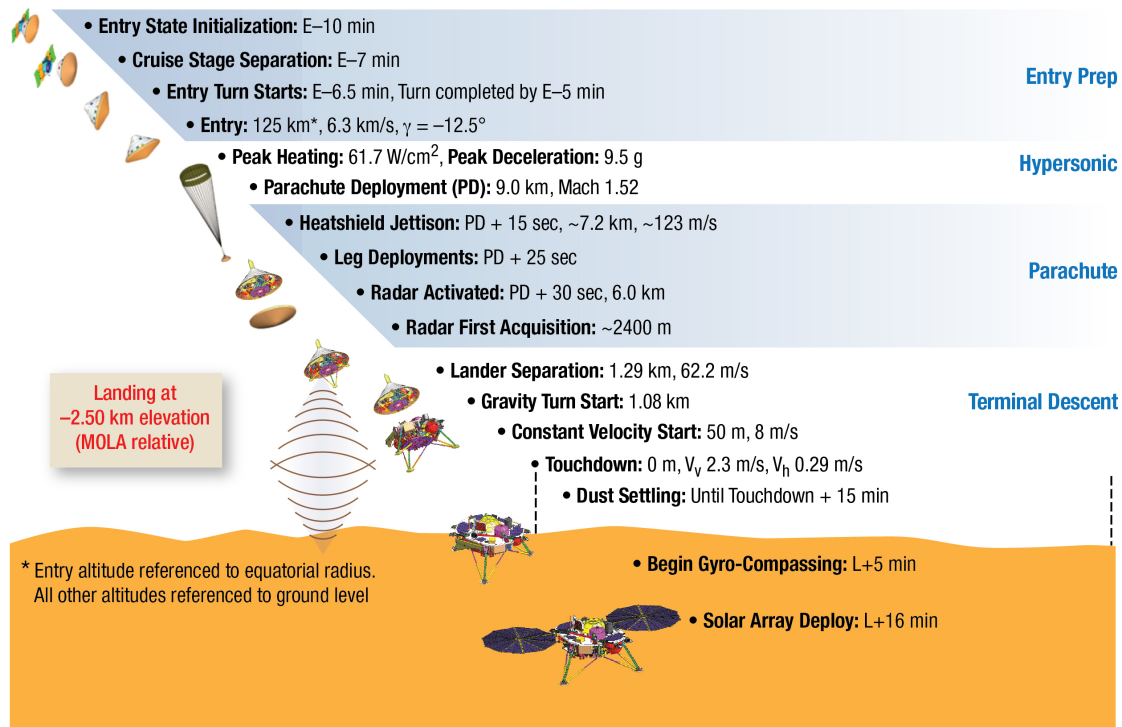


Figure 16. EDL Timeline

CONCLUSIONS

This paper has summarized the launch/arrival strategies, the Navigation and Maneuver Design, and presented results to demonstrate that all InSight Mission Design and Navigation requirements are satisfied. This strategy consists of a 23-day launch period that provides EDL communications via UHF to MRO or Direct-To-Earth. Six trajectory correction maneuvers (TCMs) are planned in order to achieve the required entry delivery accuracies.

ACKNOWLEDGMENTS

The research described in this paper was carried out at the Jet Propulsion Laboratory, California Institute of Technology, under a contract with the National Aeronautics and Space Administration. The authors would like to acknowledge the members of the InSight Mission Design and Navigation Team who performed the analyses that are reported on in this paper: Matt Golombek, Eric Graat, Tim McElrath, Fred Pelletier, and Evgeniy Sklyanskiy. The authors also acknowledge the contributions of the GNC team at Lockheed Martin. Gerard Kruijzinga and Roby Wilson served as reviewers for this paper and provided useful comments. © 2014 California Institute of Technology. Government sponsorship acknowledged.

REFERENCES

- ¹K. Fujii, "InSight Mission Plan", Preliminary, JPL D-75260, July 12, 2013.
- ²M. Wallace, "InSight Interplanetary Trajectory Characteristics Document", Preliminary, JPL D-75285, October 21, 2013
- ³M. Golombek, L. Redmond, H. Gengl, C. Schwartz, N. Warner, B. Banerdt, S. Smrekar, "Selection of the InSight Landing Site: Constraints, Plans, and Progress", *44th Lunar and Planetary Science Conference (2013)*, The Woodlands, Texas, March 18-22, 2013
- ⁴T.H. You, "InSight Navigation Plan", Preliminary, JPL D-75284, July 12, 2013
- ⁵M. Grover, B. Cichy, P. Desar, "Overview of the Phoenix Entry, Descent, and Landing System Architecture", *AIAA/AAS Astrodynamics Specialist Conference; Honolulu, HI; 18-21 Aug. 2008*